CHARACTERIZATION OF THE MICROSTRUCTURE OF YAG CERAMICS VIA STEREOLOGY-BASED IMAGE ANALYSIS

TEREZA UHLÍŘOVÁ*, JAN HOSTAŠA*,**, #WILLI PABST*

*Department of Glass and Ceramics, Institute of Chemical Technology, Prague (ICT Prague), Technická 5, 166 28 Prague 6, Czech Republic
**Institute of Science and Technology for Ceramics (CNR ISTEC), Via Granarolo 64, 48018 Faenza, Italy

#E-mail: pabstw@vscht.cz

Submitted May 12, 2014; accepted August 28, 2014

Keywords: YAG ceramics, Yb-doping, solid state lasers, microstructure, image analysis, stereology, stereological relations, grain size (mean chord length, Jeffries size), interface density (grain boundary density), mean curvature integral density, edge length density (triple junction line length density)

The microstructure of transparent YAG ceramics is investigated by stereology-based microscopic image analysis using SEM and FE-SEM micrographs. Interface densities, mean curvature integral densities and the related grain size measures (mean chord length and Jeffries size) have been determined with relative errors of 9-12 % for interface densities and mean curvature integral densities and 6-9 % for the corresponding grain size measures. A comparison of the two grain size measures confirmed an excellent linear correlation between the Jeffries size and the mean chord length, with a mean-chord-length-to-Jeffries-size ratio of 0.928 ± 0.086. The overall range of average grain sizes is approx. 11-34 μm. It has been found that the sintering time has a significant influence on the grain size, especially for YAG ceramics without Yb doping. When the sintering time is increased by a factor 8 (from 2 h to 16 h) the grain size increases by more than 200 % in undoped YAG ceramics, whereas the grain growth is much weaker in Yb-doped YAG ceramics (grain growth only 50-70 % for YAG ceramics with 5-10 at.% Yb). Thus it can be concluded that the Yb dopant acts as a grain growth inhibitor in YAG ceramics, at least for sufficiently long sintering times (8 h and more). The influence of the sintering additive (tetraethyl orthosilicate TEOS) content on the grain size is negligible in the concentration range tested (0.3-0.5 wt.%).

INTRODUCTION

Yttrium-aluminum garnet (YAG) ceramics are promising candidates for advanced optical applications, including solid state lasers [1-5]. Due to the fact that YAG is cubic (garnet structure) it is isotropic with respect to all second-order tensor properties, including refractive indices. Therefore it is an ideal material for preparing transparent ceramics, because birefringence (double refraction) at grain boundaries is not an issue [6-8]. In particular, when the porosity is sufficiently low and / or the pore size sufficiently far away from the wavelength of the electromagnetic radiation in question (e.g. visible light or near infrared radiation), it is possible to prepare YAG ceramics with a transmittance (real in-line transmittance) close to the theoretical limit of around 84.3 % [9]. On the other hand, the grain boundaries and thus the grain size may influence other properties, e.g. mechanical, thermal and thermomechanical ones, which can all play a role in determining the material behavior at higher temperatures [10,11]. While significant changes of elastic properties of ceramics are generally expected only for grain sizes in the tens-of-nanometers range [12], thermal transport properties such as thermal conductivity [13,14], as well as other mechanical properties such as strength and fracture toughness [15] may exhibit a grain size dependence at much larger grain sizes. Therefore it is generally important to know how additives such as dopants and sintering aids and processing parameters such as sintering time influence the microstructure of YAG ceramics.

The characterization of microstructures is most conveniently performed by microscopic image analysis of polished sections. This allows in principle the routine characterization of many samples in a reasonable time. Especially when the image analysis is performed on non-binarized real images in a manual manner using a superimposed grid, unbiased results can be obtained that are highly reliable and available for a clearly defined statistical evaluation. Three independent metric parameters can be obtained from such an investigation: the volume fraction (irrelevant in the case of single-phase materials), the interface density (which is related to a well-known size measure, the mean chord length) and the mean curvature integral density (which in the case of convex objects is also related to a size measure, viz. the Jeffries size). These metric parameters are accessible from two-dimensional sections (cuts), but have the same

values in the three-dimensional volume. The science to extract these volume-relevant parameters from two-dimensional sections is called stereology. While some authors determine only one of these parameters, e.g. the volume fraction or the mean chord length, the analysis can be called complete only when three independent metric parameters have been determined. This systematic stereological approach has been successfully applied to porous alumina ceramics prepared with starch [16] and to highly porous, cellular alumina ceramics prepared by yeast-mediated biological foaming [17-19].

In the present paper we apply the same approach to YAG ceramics. Since the porosity is very low in these ceramics, especially when transparent, and the ceramics are single-phase, the volume fraction is trivially (close to) unity (unless processing defects occur) and is therefore irrelevant here. In the theoretical part we give a brief summary of the stereological relations to be used and the statistical evaluation of the measured and calculated data (which are further detailed in the appendix). In the experimental part we shortly describe the processing, sample preparation and micrograph acquisition. Finally we discuss the microstructural characteristics (metric parameters) obtained, including the corresponding size measures, to elucidate the dependence of the microstructure on sintering time, Yb-dopant content and the content of the tetraethyl orthosilicate (TEOS) sintering aid.

THEORETICAL

We assume the reader to be familiar with the stereological index notation and the definitions of the basic stereological quantities volume V, surface S and mean curvature integral M [20]. In single-phase, polycrystalline materials the volume fraction V_V (dimensionless) is irrelevant, so that the only metric parameters of interest are the interface density S_V (units [mm^{-1}]), in the case of single-phase materials also called grain boundary density, and the mean curvature integral density M_V (units [mm^{-2}]), or other quantities derived from the latter two.

The interface density is determined via the Saltykov relation [21],

$$S_V = 2P_L \,, \tag{1}$$

where P_L is the number of intersection points between grain sections and probe lines (grid lines) per unit length (of the probe lines). The mean curvature integral density can be determined via the net tangent count (yielding in general the 2D Euler characteristic [20]), which in the case of simply connected objects (not necessarily convex) can be replaced by a count of objects (here grains) per unit area of the probing section (e.g. a chosen measurement frame) N_A, i.e. by the relation [20],

$$M_V = 2\pi \cdot N_A \,. \tag{2}$$

The mean chord length[1] of grains $\bar{L}$, which is a dimension-invariant measure of the grain size, is related (inversely proportional) to the interface density S_V and calculated via the relation [22]

$$\bar{L} = \frac{2}{S_V} = \frac{1}{P_L} \quad . \tag{3}$$

Similarly, the Jeffries size of the grain sections (Jeffries grain size [21]) is related to the mean curvature integral density and can be calculated via the relation

$$J = \sqrt{\frac{2\pi}{M_V}} = \sqrt{\frac{1}{N_A}} \quad . \tag{4}$$

The physical meaning of the Jeffries size[2], which is intimately related to the "ASTM grain size number" [23], is the edge length of an "average" square, the area of which equals the area of an "average" grain section (more precisely, a number-weighted arithmetic mean section area), because the mean section area is defined as

$$\bar{A} = \frac{1}{N_A} \quad . \tag{5}$$

Since the area of a circle equals the product of mean chord length and diameter, the ratio $\bar{L}/J$ for monodisperse circular sections would be 0.886 [23]. However, higher values of this ratio are expected [23] and have been found for polycrystalline microstructures with polydisperse grains, e.g. 0.935 [24].

On the other hand, it is well known that for polyhedral grains with straight edges the grain count per unit area can be replaced by a triple point count, since the number of intersection points of triple junctions with the section plane (per unit area of the section plane) equals twice the number of grain sections (per unit area of the section plane) [21], i.e.

$$P_A = 2N_A \,. \tag{6}$$

However, at the same time, the areal triple point density is related to the volumetric edge line density [25], i.e.

$$L_V = 2P_A \,. \tag{7}$$

Therefore it can be said that for polycrystalline microstructures with polyhedral grains the Jeffries size J is a grain size measure based on the triple junction length per unit volume (edge length density) L_V, while the mean chord length is a grain size measure based on the grain boundary area per unit volume (interface density) S_V. It has to be emphasized that the two grain size measures are principally independent, and depending on the application in mind, either one or the other may be more appropriate. Since most effective properties of heterogeneous materials are more affected by the interfaces than by triple junctions, the mean chord length is the more common choice, of course.

[1] *The mean chord length is also called "mean intercept length" [23].*
[2] *The Jeffries size is sometimes – misleadingly – called "mean section diameter" [23].*

The absolute error of all these microstructural parameters (here denoted x) can be calculated from the standard error (= standard deviation of the cumulative sample mean) and the normalized deviation (also called "t-variate") according to the so-called Student t-distribution, which determines the reliability of the result, i.e. the probability with which the true population mean is expected to lie within the confidence intervals around the (cumulative) sample mean. Thus the absolute error corresponding to 95 % reliability is generally given by the relation

$$\Delta x = t_{0.95}(n) \cdot \sigma(\langle x \rangle) , \quad (8)$$

where $\sigma(\langle x \rangle)$ is the standard error of the cumulative sample mean $\langle x \rangle$ and $t_{0.95}(n)$ the normalized deviation for 95 % reliability, with the argument n denoting the so-called "degrees of freedom", which are related to the number of measurements in each sample, i.e. the number of intersection points between grain section outlines and grid lines ($n = P_{intersection} - 1$), the number of grain sections counted ($n = N_{grain} - 1$) or the number Y of samples, i.e. grids, measurement frames or micrographs ($n = Y - 1$) [19].

Generally, after the measurements have been performed, the standard error can be calculated from the usual standard deviation $\sigma(x)$ via the relation

$$\sigma(\langle x \rangle) = \frac{\sigma(x)}{\sqrt{Y}} , \quad (9)$$

where Y is the number of samples and $\sigma(x)$ is the usual standard deviation

$$\sigma(x) = \sqrt{\frac{\sum (x_i - \langle x \rangle)^2}{Y - 1}} , \quad (10)$$

where x_i are the individual sample means (usually based on many single measurements in one sample) [19].

Additionally, it is possible to estimate the standard error directly from the (cumulative) number of single measurements (if necessary before the measurements are made, e.g. to determine in advance the necessary number of measurements to be made). In particular, the standard error of the interface density S_V is determined by the relation [19,21]

$$\sigma(S_V) = k_1 \cdot \frac{S_V}{\sqrt{P_{intersection}}} , \quad (11)$$

where $P_{intersection}$ is the number of intersection points of grid lines with grain section outlines and k_1 is an empirical factor, whose values are reported to range from approximately 0.5 to 1.5 [21] or even 2.0 [22], but sometimes the value 0.65 is preferred [24]. In this contribution we set $k_1 = 1$, see the discussion in [21]. Similarly, the standard error of the mean curvature integral density M_V can be calculated from an empirical relation of the same type, i.e.

$$\sigma(M_V) = k_2 \cdot \frac{M_V}{\sqrt{N_{grain}}} , \quad (12)$$

where $N_{section}$ is the number of grain sections counted and k_2 is an empirical constant, whose value is reported to be 1.03 [24]. In this contribution we set $k_2 = 1$, see the discussion in [21]. The expected standard errors of the mean chord length and the Jeffries size follow from those of S_V and M_V by application of the law of error propagation, i.e.

$$\sigma(\bar{L}) = \frac{\bar{L}}{\sqrt{P_{intersection}}} , \quad (13)$$

$$\sigma(J) = \frac{J}{2\sqrt{N_{grain}}} \quad (14)$$

(note that the relative error of the Jeffries size is only half that of the mean curvature integral density, because J is inversely proportional not to M_V itself but to its square root). Observed and expected errors are usually very similar. For reasons of simplicity all errors cited in the main text of this paper are arithmetic means of the observed errors and the expected errors, corresponding to 95 % confidence intervals, see Appendix A. Relative errors are calculated by dividing these absolute errors by the corresponding mean values.

EXPERIMENTAL

Powder processing

The YAG ceramics in this work have been prepared from commercially available oxide powders with purity > 99.99 %: Al_2O_3 with D_{50} = 0.2 µm (Taimei DS-6), Y_2O_3 with D_{50} = 0.05 µm (Nanocerox) and Yb_2O_3 with D_{50} = 5.6 µm (Alfa Aesar Reacton). The composition of prepared samples was YAG with 0, 5 and 10 at.% of Yb, i.e. from $Y_3Al_5O_{12}$ to $Y_{2.7}Yb_{0.3}Al_5O_{12}$. Tetraethyl orthosilicate (TEOS, 99.999 %, Sigma Aldrich) was used as a sintering aid in amounts of 0.3-0.5 wt.% (with respect to solid mass). Powders were mixed and homogenized by ball milling with with alumina balls in ethanol for 72 h, using polyalkylene glycol (Zschimmer & Schwarz KM 5140) as a dispersant, and subsequently spray dried. For further processing details the reader may refer to a previous publication [26].

Sample preparation and microscopy

Disk-shaped samples with diameter 15 mm and a few mm in thickness were prepared by uniaxial pressing the spray-dried granules, followed by isostatic pressing at 250 MPa and solvent removal in air at 600 °C. Sintering was performed in a W-Mo-furnace in high vacuum at a temperature of 1735 °C for 2, 8 and 16 h (in one case also 24 h). After sintering, the samples were annealed in air for 100 h at 1100 °C, in order to eliminate oxygen vacancies and allow Yb^{2+} to re-oxidize to Yb^{3+}, see also [26]. After sintering and annealing the samples were polished to obtain flat surfaces. SEM micrographs were

recorded from thermally etched sections using a Leica Cambridge Stereoscan 360. Alternatively, an SEM with field-emission gun (FE-SEM, Carl Zeiss Sigma) has been used in some cases to acquire images by grain orientation contrast from polished sections without thermal etching.

RESULTS AND DISCUSSION

Sample types and microstructural parameters

Table 1 lists the numbers of samples and micrographs evaluated and the total numbers of intersection points and objects counted for different types of YAG ceramics (firing temperature 1735 °C) in dependence on the Yb dopant contents (0, 3, 5, 7 and 10 at.%), TEOS contents (0.3 and 0.5 wt.%) and firing time (2, 8, 16 and 24 h). Of each sample type 1-3 samples were characterized based on 3-14 SEM micrographs. Examples of the SEM micrographs used are shown in Figure 1. Depending on the sample type, 156-2212 intersection points and 166-1937 objects (grain sections) were counted and the resulting numbers divided by the length of probe lines (horizontal and vertical grid lines) and the area of the measurement frame (grid area), yielding the stereological parameters P_L and N_A, respectively.

Table 2 lists the microstructural parameters calculated from the stereological parameters P_L and N_A,

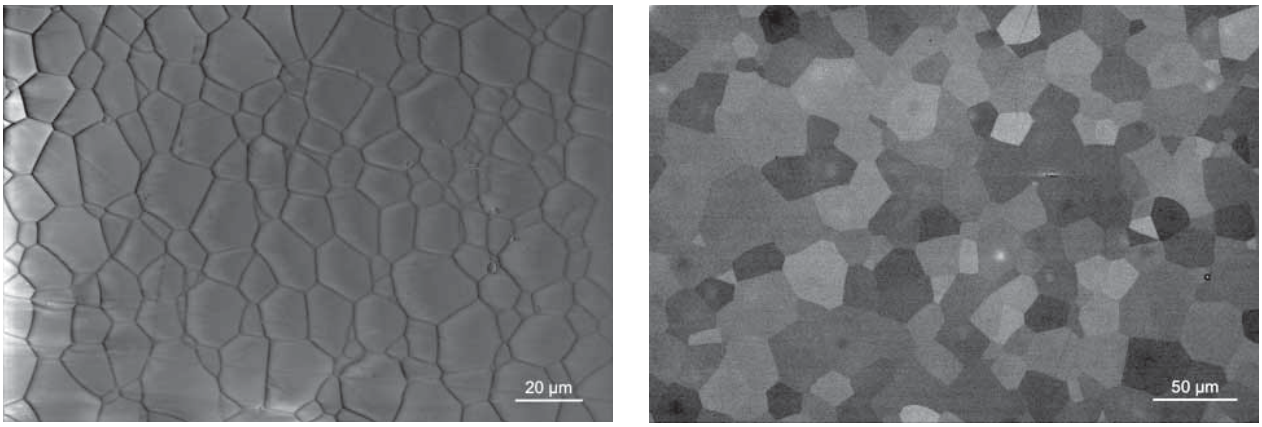

a) b)

Figure 1. Micrographs of transparent YAG ceramics with 0.5 wt.% TEOS as a sintering aid fired at 1735 °C; a) SEM micrograph of undoped YAG sintered for 2 h, b) FE-SEM micrograph of YAG doped with 5 at.% Yb sintered for 8 h.

Table 1. Number of samples and micrographs evaluated and total number of intersection points and objects (grain sections) counted for YAG ceramics (firing temperature 1735 °C) in dependence of Yb dopant contents of (0, 3, 5, 7 and 10 at.%), TEOS contents (0.3 and 0.5 wt.%) and firing time (2, 8, 16 and 24 h).

Yb content (at.%)	TEOS content (wt.%)	Firing time (h)	Number of samples	Number of micrographs evaluated	Total number of intersection points counted	Total number of grain sections counted
0	0.5	2	1	13	2212	1937
0	0.5	8	1	6	657	659
0	0.5	16	1	6	450	366
3	0.5	16	1	6	475	395
5	0.5	2	1	12	1473	1064
5	0.5	8	2	8 + 6 = 14	873 + 537 = 1410	1076 + 524 = 1600
5	0.3	16	3	5 + 3 +3 = 11	381 + 121 + 406 = 908	436 + 127 + 469 = 1032
5	0.5	16	2	5 + 2 = 7	321 + 145 = 466	326 + 164 = 490
5	0.5	24	1	3	156	197
7	0.5	16	1	6	373	253
10	0.5	2	1	11	763	372
10	0.3	8	1	6	581	592
10	0.5	8	1	9	694	595
10	0.3	16	2	4 + 5 = 9	176 + 296 = 472	125 +387 = 512
10	0.5	16	1	6	282	166
Range of numbers	–	–	1-3	3-14	156-2212	166-1937

including the absolute errors for each sample type. The absolute errors in this table are arithmetic averages of observed and estimated errors corresponding to the 95 % confidence interval according to the Student *t*-distribution. A detailed comparison of observed and estimated errors is given in Appendix A. In the case of separately evaluated multiple samples (specimens) of one sample type both the mean values of the microstructural parameters and their errors have been averaged.

An overall inspection of the values in Table 2 shows that the average grain sizes determined in this work for YAG ceramics are in the range from approx. 10-11 μm to 33-35 μm. The corresponding interface densities are 61-207 mm^{-1} and the mean curvature integral densities range from approx. 5080 to more than 52800 mm^{-2} (corresponding edge line densities are 7980-83000 mm^{-2}). These values may be compared to interface densities in the range 16-192 mm^{-1} and mean curvature integral densities in the range 860-35700 mm^{-2} for porous ceramics prepared with corn and potato starch using a pore former and pore sizes (mean chord lengths) in the range 8-27 μm [16]. The relative errors of the parameters are largest for the mean curvature density (8-20 %) and smallest for the Jeffries size (4-10 %). Since the Jeffries size is related to the square root of the mean curvature density, it is not surprising that the relative errors of the former are approximately one half of those of the latter. The average relative error is 9-12 % for the interface densities and mean curvature integral densities and slightly lower, namely 6-9 %, for the corresponding grain size measures.

Dependence of YAG ceramics microstructure on the Yb dopant content

Figure 2 shows the interface density S_V (= volumetric grain boundary area density) and the mean curvature integral density M_V of dense (porosity orders of magnitude below 1 %), transparent polycrystalline Yb-doped yttrium-aluminum-garnet (YAG) ceramics fired at 1735 °C for 2 h. Figure 3 shows the corresponding grain size measures, viz. the mean chord length $\bar{L}$ and the Jeffries size *J*. It can be seen that the mean chord length is always slightly lower than the Jeffries size. However, both parameters seem to represent consistent measures of grain size, see below.

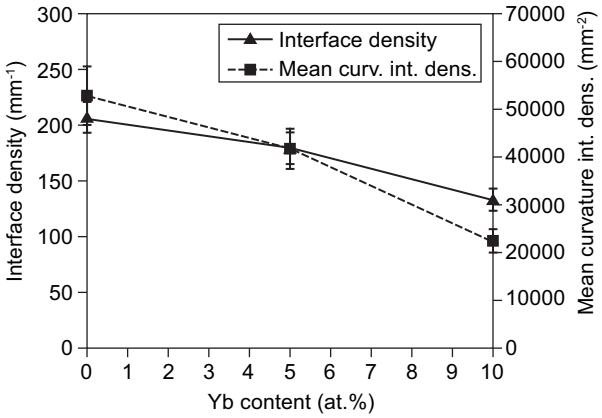

Figure 2. Interface density (= grain boundary density) and mean curvature integral density of dense transparent polycrystalline Yb-doped YAG ceramics; TEOS content 0.5 wt.%, firing temperature 1735 °C, firing time 2 h.

Table 2. Microstructural parameters of YAG ceramics (firing temperature 1735 °C) in dependence of Yb dopant contents of (0, 3, 5, 7 and 10 at.%), TEOS contents (0.3 and 0.5 wt.%) and firing time (2, 8 16, 24 h); errors correspond to 95 % confidence intervals.

Yb content (at.%)	TEOS content (wt.%)	Firing time (h)	S_V (mm^{-1})	M_V (mm^{-2})	Mean chord length (μm)	Jeffries size (μm)	Ratio $\bar{L}/J$ (–)
0	0.5	2	207.1 ± 13.8	52846 ± 6122	9.9 ± 0.6	11.3 ± 0.6	0.877 ± 0.027
0	0.5	8	104.3 ± 7.1	12780 ± 1236	19.3 ± 1.3	22.3 ± 1.1	0.864 ± 0.055
0	0.5	16	60.6 ± 5.0	5081 ± 617	33.2 ± 2.7	35.5 ± 2.1	0.938 ± 0.068
3	0.5	16	113.1 ± 9.4	17235 ± 1508	17.8 ± 1.5	19.2 ± 0.9	0.930 ± 0.065
5	0.5	2	179.3 ± 14.2	41722 ± 4207	11.5 ± 0.9	12.5 ± 0.6	0.913 ± 0.044
5	0.5	8	94.6 ± 6.8	12906 ± 1166	21.6 ± 1.5	22.6 ± 0.9	0.953 ± 0.037
5	0.3	16	104.6 ± 13.8	14689 ± 2909	19.4 ± 2.5	21.2 ± 2.0	0.916 ± 0.051
5	0.5	16	104.3 ± 12.2	14190 ± 1900	19.5 ± 2.1	21.2 ± 1.4	0.918 ± 0.246
5	0.5	24	74.3 ± 6.7	8596 ± 1320	26.9 ± 2.4	27.2 ± 2.1	0.995 ± 0.201
7	0.5	16	88.8 ± 11.3	11039 ± 1280	23.3 ± 3.2	24.0 ± 1.4	0.963 ± 0.146
10	0.5	2	133.2 ± 9.9	22438 ± 2445	15.2 ± 1.1	16.9 ± 0.9	0.906 ± 0.094
10	0.3	8	138.3 ± 9.3	25831 ± 2773	14.5 ± 1.0	15.7 ± 0.8	0.926 ± 0.066
10	0.5	8	110.2 ± 7.8	17308 ± 1423	18.4 ± 1.4	19.2 ± 0.8	0.956 ± 0.055
10	0.3	16	113.6 ± 13.3	17944 ± 2526	18.2 ± 2.1	19.3 ± 1.4	0.938 ± 0.066
10	0.5	16	85.4 ± 6.7	9788 ± 1148	23.5 ± 1.8	25.4 ± 1.5	0.925 ± 0.068
Relative error (%) (range)			6.7-13.2	8.2-19.8	6.2-13.7	3.9-9.6	3.8-26.8
Relative error (%) (average)			8.8	11.8	8.7	5.8	9.2

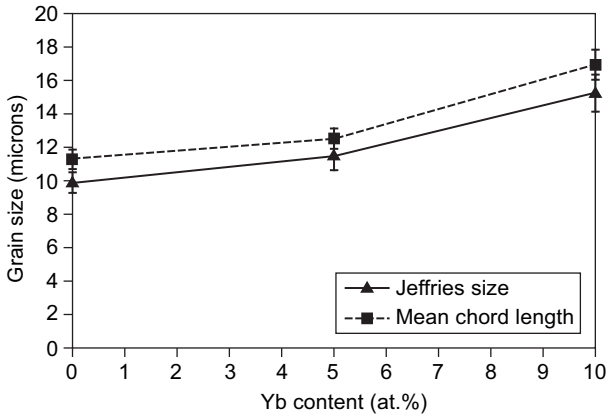

Figure 3. Grain size (mean chord length and Jeffries size) of dense transparent polycrystalline Yb-doped YAG ceramics; TEOS content 0.5 wt.%, firing temperature 1735 °C, firing time 2 h.

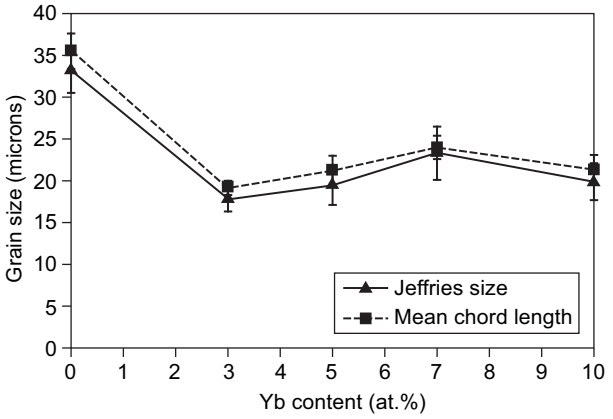

Figure 5. Grain size of YAG ceramics as a function of the Yb content; TEOS content 0.3-0.5 wt.%, firing temperature 1735 °C, firing time 16 h.

From Figure 3 it is evident that after two hours of sintering the grain size increases slightly with Yb dopant content, viz. from 9.9-11.3 μm (mean chord length and Jeffries size, respectively) for samples without Yb to 11.5-12.5 μm for samples with 5 at.% Yb and 15.2-16.9 μm for samples with 10 at.% Yb. Thus the grain size after 2 h sintering is higher by 54-49 % for YAG doped with 10 at.%, compared to the undoped material. The interface densities and mean curvature integral densities are correspondingly lower, showing a decrease with increasing Yb dopant content, see Figure 2.

Interestingly, however, the situation changes completely for longer sintering times, e.g. 16 h, see Figures 4 and 5. In this case the grain size for Yb-doped samples is much smaller than that of the undoped materials. This finding may be explained by a solute drag mechanism preventing grain growth. Nevertheless, the different behavior for different sintering times seems to be paradoxical at first sight, and actually the ultimate reason for this difference is not clear. What can be said, however, is that the sintering time has a far more significant influence on the microstructure (grain size) than the Yb content.

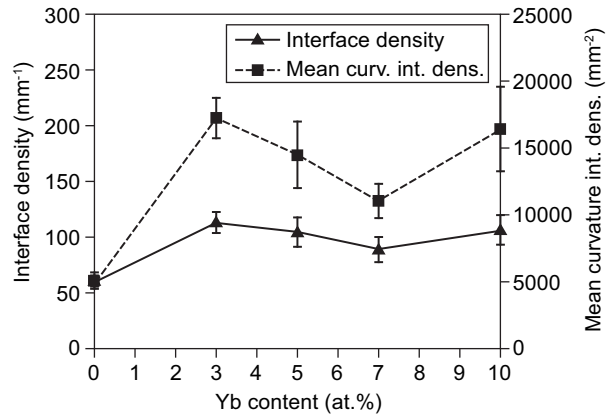

Figure 4. Interface density and mean curvature integral density of YAG ceramics as a function of the Yb content; TEOS content 0.3-0.5 wt.%, firing temperature 1735 °C, firing time 16 h.

Dependence of YAG ceramics microstructure on the sintering time

Figures 6 through 11 show the interface densities, mean curvature integral densities and the corresponding grain size measures (mean chord length and Jeffries size) in dependence of the firing or sintering time (for a sintering temperature of 1735 °C). Obviously, with prolongued sintering time the grain size increases in all cases, as expected. Moreover, it is evident that YAG ceramics without Yb doping exhibit the strongest grain growth (from 9.9-11.3 μm to 33.2-35.5 μm, i.e. to values more than thrice the original values, corresponding to an increase of 214-235 %), when the sintering time is increased from 2 h to 16 h, i.e. by a factor of 8 (i.e. almost one order of magnitude). By contrast, YAG ceramics with 5 or 10 at.% Yb doping exhibit a much weaker grain growth, from 11.5-12.5 μm to 19.5-21.2 μm and from 15.2-16.9 μm to 23.5-25.4 μm, corresponding to values less than twice the original ones, i.e. grain size values corresponding to an increase of only 70 % and 50-52 %, respectively, for the same range of sintering times. This demonstrates quite nicely the grain-growth inhibiting effect of Yb-doping. However, as mentioned before (see Figure 3), sufficiently long sintering times are required for this effect to be pronounced.

Dependence of YAG ceramics microstructure on the sintering additive content

Figures 12 and 13 show the interface densities, mean curvature integral densities and the corresponding grain size measures (mean chord length and Jeffries size) of YAG ceramics with 5 and 10 at.% Yb doping in dependence of the content of tetraethyl orthosilicate (TEOS), which has been used as a sintering additive (here either 0.3 or 0.5 wt.%). Corresponding data for YAG ceramics with 0.5 wt.% TEOS but without Yb doping are shown for comparison. The sintering temperature is 1735 °C and the sintering time 16 h in all cases.

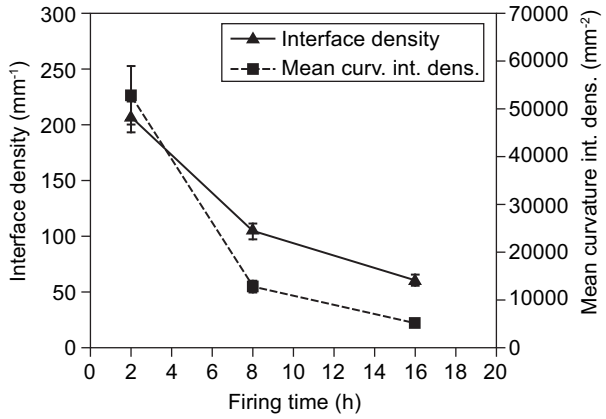

Figure 6. Interface density and mean curvature integral density of YAG ceramics without Yb doping as a function of the firing time (firing temperature 1735 °C, Yb content 0 at.%, TEOS content 0.5 wt.%).

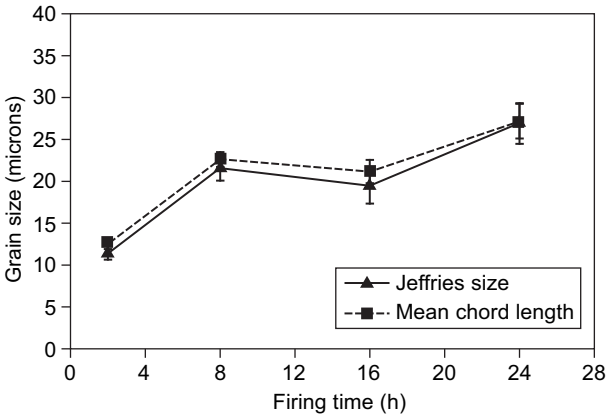

Figure 9. Grain size of YAG ceramics with Yb doping as a function of the firing time (firing temperature 1735 °C, Yb content 5 at.%, TEOS content 0.5 wt.%).

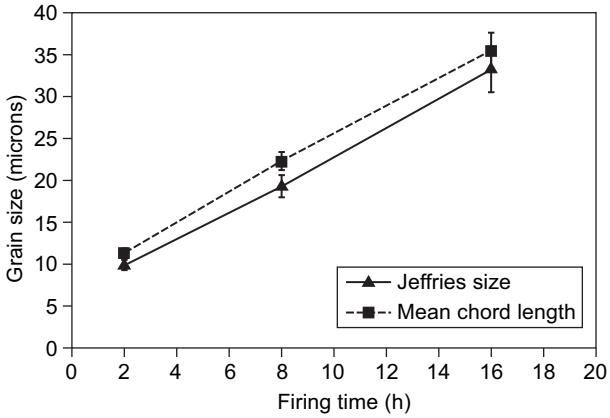

Figure 7. Grain size of YAG ceramics without Yb doping as a function of the firing time (firing temperature 1735 °C, Yb content 0 at.%, TEOS content 0.5 wt.%).

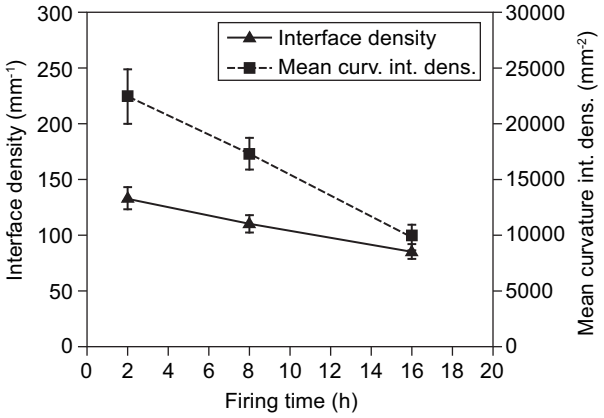

Figure 10. Interface density and mean curvature integral density of YAG ceramics with Yb doping as a function of the firing time (firing temperature 1735 °C, Yb content 10 at.%, TEOS content 0.5 wt.%).

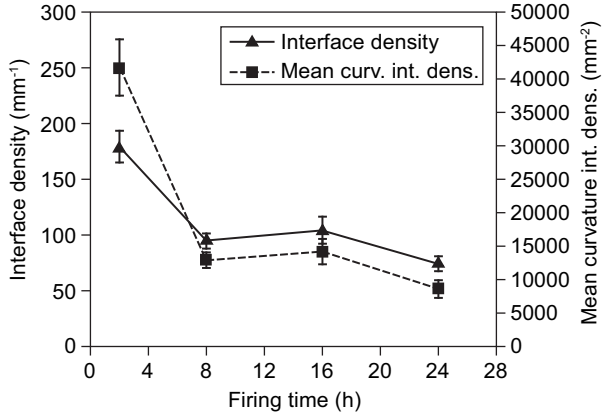

Figure 8. Interface density and mean curvature integral density of YAG ceramics with Yb doping as a function of the firing time (firing temperature 1735 °C, Yb content 5 at.%, TEOS content 0.5 wt.%).

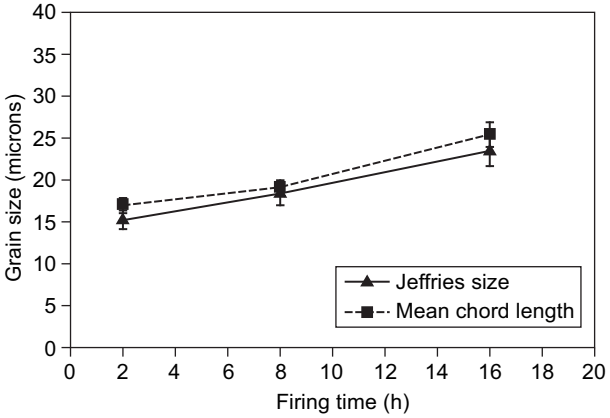

Figure 11. Grain size of YAG ceramics with Yb doping as a function of the firing time (firing temperature 1735 °C, Yb content 10 at.%, TEOS content 0.5 wt.%).

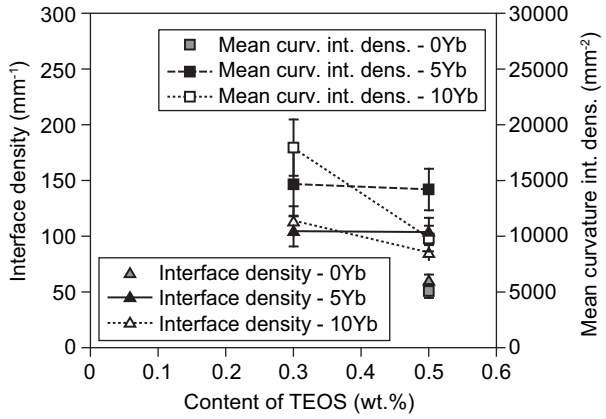

Figure 12. Interface density and mean curvature integral density of YAG ceramics as a function of the sintering additive (TEOS) content (sintering temperature 1735 °C, sintering time 16 h).

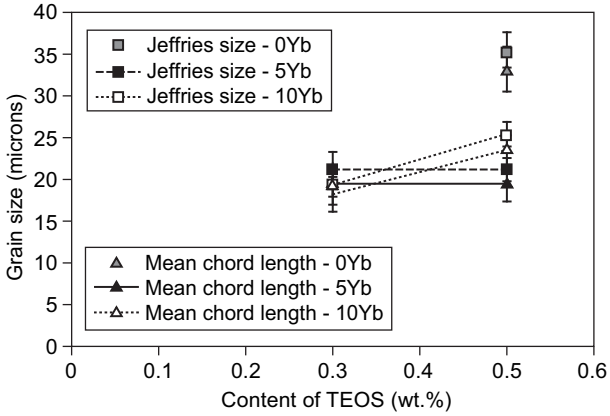

Figure 13. Grain size of YAG ceramics as a function of the sintering additive (TEOS) content (sintering temperature 1735 °C, sintering time 16 h).

According to these results, based on the two TEOS concentrations used (0.3 and 0.5 wt.%), the influence of TEOS on the grain size does not seem to be very significant. It is clear, however, that this finding does not allow conclusions that go beyond this concentration range.

Correlation between mean chord length and Jeffries size

Figure 14 shows the correlation between the Jeffries size and the mean chord length. From this figure and the values in Table 2 it is evident that there is a clear correlation between the two grain size measures and that the ratio $\bar{L}$ /J is always close to – but slightly smaller than – unity, the overall average of the ratio $\bar{L}$ /J being 0.928 ± 0.086. That means, for the YAG ceramics investigated in this paper, the mean chord length is always slightly smaller than the Jeffries size. However, it can be said that both grain size measures, the size measure $\bar{L}$ derived from the interface density (volumetric grain boundary area density) as well as the size measure J derived from the mean curvature integral density, in other words the size measure related to the volumetric grain edge density, exhibit an excellent linear correlation and provide a mutually consistent description of grain size.

It should be recalled, that, similar to the Jeffries size, also the so-called ASTM grain size number is based on the volumetric grain edge density (since also the latter is calculated from the measured parameter N_A). The ASTM grain size numbers for the materials investigated in this paper are in the range 6.5-10, corresponding to mean chord lengths in the range 10-33 μm and Jeffries sizes in the range 11-35 μm.

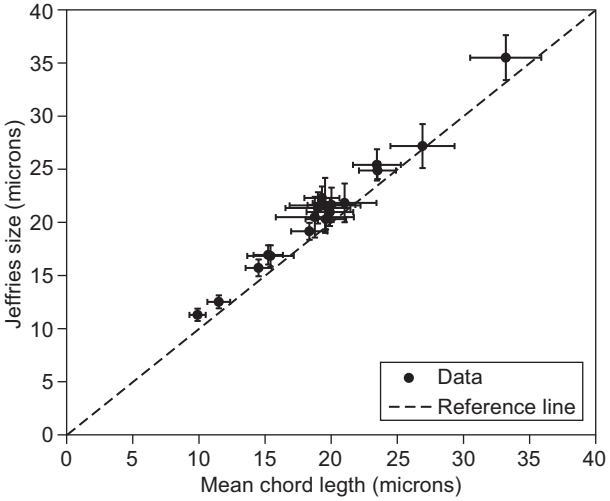

Figure 14. Correlation between Jeffries size and mean chord length.

CONCLUSIONS

The microstructure of transparent YAG ceramics has been investigated by stereology-based microscopic image analysis using SEM and FE-SEM micrographs of polished sections prepared with or without thermal etching, respectively. Interface densities, mean curvature integral densities and the related grain size measures (mean chord length and Jeffries size) have been determined via point or object counting methods using rectangular grids or measurement frames. The number of points or objects per sample type ranged from approx. 160 to more than 2000, depending on the number of micrographs available and the grain size. Apart from the mean values determined, absolute and relative errors were calculated using the Student distribution, based on observed standard deviations and on estimated standard errors. On the average, relative errors are 9-12 % for interface densities and mean curvature integral densities and slightly smaller, 6-9 % for the corresponding grain size measures.

A comparison of the two grain size measures confirmed an excellent linear correlation between the Jeffries size and the mean chord length, with an $\bar{L}/J$ ratio of 0.928 ± 0.086. This value may be considered as a significant characteristic parameter of the microstructure of the YAG ceramics prepared. Further, it has been found that the sintering time has a significant influence on the grain size, especially for YAG ceramics without Yb doping. When the sintering time is increased by a factor 8 (from 2 h to 16 h) the grain size increases by more than 200 % (i.e. to more than thrice the original value) in undoped YAG ceramics, whereas the grain growth is much weaker in Yb-doped YAG ceramics (grain size increase only 50-70 % for YAG ceramics with 5-10 at.% Yb). Thus it can be concluded that the Yb dopant acts as a grain growth inhibitor in YAG ceramics, probably via a solute drag mechanism. However, results for short sintering times (2 h) indicate that the grain growth inhibiting effect of Yb dopants is working only for sufficiently long sintering times (8 h and more). Results for two (similar) concentrations of sintering additive (TEOS) indicate that the influence of the TEOS content on the grain size is negligible, at least in the concentration range tested (0.3-0.5 wt.%).

The overall range of average grain sizes is approx. 11-34 μm, corresponding to interface densities in the range approx. 60-210 mm^{-1} and mean curvature integral densities in the range approx. 5000-53000 mm^{-2} (or edge line densities in the range approx. 8000-83000 mm^{-2}). For such large grains (and correspondingly low interface densities and mean curvature integral densities or edge line densities) it is clear that any grain size effects on the elastic properties and thermal conductivity can be with certainty excluded. Thus, the elastic and thermal properties of these polycrystalline ceramics will essentially correspond to the averaged tensor components of the corresponding crystallite properties and can thus be predicted from the bulk properties of YAG monocrystals. Since YAG crystallites are cubic and therefore optically isotropic (at least with respect to linear optical phenomena such as refraction) due to the absence of birefringence (double refraction), the grain size itself should have no effect on the optical properties at all. Therefore the optical properties, including transparency, will depend solely on the porosity, pore size (distribution) and pore shape (distribution) and the cleanness of the interfaces. The optimization of composition and processing should therefore mainly be focussed towards achieving lowest porosity and clean interfaces, while grain size itself seems to be rather uncritical from the viewpoint of properties and application behavior. Only strength and related mechanical properties (e.g. fracture toughness) might be slightly improved by keeping the grain size small.

Appendix A. Comparison of observed and estimated errors

Tables A1 and A2 list the observed and estimated absolute errors and their ratios for different microstructural parameters of YAG ceramics (firing temperature

Table A1. Observed and estimated absolute errors and their ratios for different microstructural parameters of YAG ceramics (firing temperature 1735 °C) in dependence of Yb dopant contents of (0, 3, 5, 7 and 10 at.%), TEOS contents (0.3 and 0.5 wt.%) and firing time (2, 8 16, 24 h); errors correspond to 95 % confidence intervals and have been averaged in the case of (independently measured) multiple samples of the same type.

Yb content (at.%)	TEOS content (wt.%)	Firing time (h)	Observed error of S_V (mm^{-1})	Estimated error of S_V (mm^{-1})	Observed error of $\bar{L}$ (μm)	Estimated error of $\bar{L}$ (μm)	Average ratio of observed and estimated errors
0	0.5	2	19.05	8.63	0.82	0.41	2.10
0	0.5	8	6.12	7.99	1.16	1.48	0.78
0	0.5	16	4.34	5.61	2.29	3.08	0.76
3	0.5	16	8.65	10.20	1.38	1.61	0.85
5	0.5	2	19.30	9.16	1.13	0.59	2.01
5	0.5	8	6.55	7.07	1.29	1.65	0.86
5	0.3	16	14.33	13.27	2.53	2.43	1.06
5	0.5	16	10.12	14.19	1.55	2.68	0.65
5	0.5	24	1.63	11.75	0.59	4.26	0.14
7	0.5	16	13.56	9.04	4.00	2.37	1.59
10	0.5	2	10.39	9.47	1.14	1.08	1.08
10	0.3	8	7.30	11.27	0.79	1.18	0.66
10	0.5	8	7.37	8.21	1.38	1.37	0.95
10	0.3	16	11.87	14.64	1.73	2.45	0.76
10	0.5	16	3.30	10.01	0.87	2.75	0.32
Average ratio (range)							0.14-2.10
Grand average of average ratios							0.97

Table A2. Observed and estimated absolute errors and their ratios for different microstructural parameters of YAG ceramics (firing temperature 1735 °C) in dependence of Yb dopant contents of (0, 3, 5, 7 and 10 at.%), TEOS contents (0.3 and 0.5 wt.%) and firing time (2, 8 16, 24 h); errors correspond to 95 % confidence intervals and have been averaged in the case of (independently measured) multiple samples of the same type.

Yb content (at.%)	TEOS content (wt.%)	Firing time (h)	Observed error of M_V (mm^{-1})	Estimated error of M_V (mm^{-1})	Observed error of J (μm)	Estimated error of J (μm)	Average ratio of observed and estimated errors
0	0.5	2	9890	2354	0.91	0.25	3.92
0	0.5	8	1495	978	1.30	0.85	1.53
0	0.5	16	713	522	2.41	1.82	1.34
3	0.5	16	1312	1705	0.75	0.95	0.78
5	0.5	2	5905	2510	0.84	0.38	2.28
5	0.5	8	1429	904	0.94	0.84	1.35
5	0.3	16	4038	1780	2.82	1.27	2.25
5	0.5	16	1849	1951	1.40	1.39	0.98
5	0.5	24	1432	1208	2.22	1.91	1.17
7	0.5	16	1194	1367	1.31	1.49	0.88
10	0.5	2	2603	2288	0.94	0.86	1.12
10	0.3	8	3461	2085	0.95	0.63	1.58
10	0.5	8	1453	1394	0.83	0.77	1.06
10	0.3	16	2744	2309	1.45	1.39	1.12
10	0.5	16	796	1500	1.00	1.95	0.52
Average ratio (range)							0.52-3.92
Grand average of average ratios							1.46

1735 °C) in dependence of Yb dopant contents (0, 3, 5, 7 and 10 at.%), TEOS contents (0.3 and 0.5 wt.%) and firing time (2, 8 16, 24 h). With respect to the fact that the mean chord length is intimately related to the interface density (volumetric grain boundary area density), their error ratios (see Table A1) are very similar, as expected. The same holds for the Jeffries size and the mean curvature integral density (see Table A2). Therefore it is justified to consider only the arithmetic average of the ratios of observed and estimated errors in either group of parameters (errors of S_V and $\overline{L}$ on the one hand and errors of M_V and J on the other). On the other hand, with respect to the fact that the relative errors of quantities based on P_L and N_A are different, it seems appropriate to list the results in two different tables.

It is evident that the observed errors are in the majority of cases smaller than or approximately equal to the estimated ones (ratio values of around 1 and smaller). Only in 3-5 out of 15 sample types the ratio of observed and estimated errors exceeds a value of 1.5 and only in 2-3 cases out of 15 it exceeds a value of 2. This indicates that in the majority of cases the measurements are more precise than expected from the theory of statistics. When the observed errors are significantly higher than the estimated ones this is an indication either that the number of independent measurements (micrographs) was too small (so that the *t*-variate of the Student distribution blows up the error) or that the samples are non-uniform, i.e. the micrographs of one sample exhibit considerable differences (so that the standard deviation becomes very large). The latter seems to be the case on the majority of cases here. On the other hand, it is clear that in individual cases the observed error can be significantly lower than the estimated ones, just accidentally. In this case the observed error would indicate an exaggerated precision. Therefore and for reasons of simplicity in the main text of this paper we have decided to use the arithmetic average of the observed and estimated errors as the final error value used in all tables and graphs. With respect to the foregoing this value can be considered as a conservative (i.e. "worst-case") estimate of the error in the majority of cases.

Acknowledgement

This work was part of the projects A2_FCHT_2014_068 and A1_FCHT_2014_006, supported within specific university research by the Czech Ministry of Education, Youth and Sports (MŠMT No. 20/2014) and of the project P108/12/1170, supported by the Czech Science Foundation (GAČR). Support is gratefully acknowledged.

REFERENCES

1. Ikesue A., Kinoshita T., Kamata K., Yoshida K.: J. Am. Ceram. Soc. *78*, 1033 (1995).
2. Lupei V., Lupei A., Ikesue A.: Opt. Mater. *30*, 1781 (2008).

3. Esposito L., Epicier T.,Serantoni M., A. Piancastelli, Alderighi D., Pirri A., Toci G., Vannini M., Anghel S., Boulon G.: J. Eur. Ceram. Soc. *32*, 2273 (2012).
4. Sanghera J., Kim W., Villalobos G., Shaw B., Baker C., Frantz J., Sadowski B., Aggarwal I.: Opt. Mater. *35*, 693 (2013).
5. Cavalli E., Esposito L., Hostaša J., Pedroni M.: J. Eur. Ceram. Soc. *33*, 1425 (2013).
6. Apetz R., van Bruggen M. P. B.: J. Am. Ceram. Soc. *86*, 480 (2003).
7. Krell A., Hutzler T., Klimke J.: J. Eur. Ceram. Soc. *29*, 207 (2009).
8. Klimke J., Trunec M., Krell A.: J. Am. Ceram. Soc. *94*, 1850 (2011).
9. Pabst W., Hostaša J., Esposito L.: J. Eur. Ceram. Soc. *34*, 2745 (2014).
10. Hostaša J., Matějíček J., Nait-Ali B., Smith D. S., Pabst W., Esposito L.: J. Am. Ceram. Soc. *97*, 2602 (2014).
11. Ferrara P., Ciofini M., Esposito L., Hostaša J., Labate L., Lapucci A., Pirri A., Toci G., Vannini M., Gizzi L. A.: Optics Express *22*, 5375 (2014).
12. Pabst W., Gregorová E.: *Phase Mixture Models for the Properties of Nanoceramics*, p. 1-69, Nova Science Publishers, New York 2010.
13. Fayette S., Smith D. S., Smith A., Martin C.: Influence of grain size on the thermal conductivity of tin oxide ceramics, *J. Eur. Ceram. Soc. 20*, 297 (2000).
14. Pabst W., Hostaša J.: Thermal conductivity of ceramics: from monolithic to multiphase, from dense to porous, from micro to nano, in: *Advances in Materials Science Research – Volume 7*, p. 1-112, Ed. Wythers M. C., Nova Science Publishers, New York 2011.
15. Rice R. W.: *Mechanical Properties of Ceramics and Composites – Grain and Particle Effects*, p. 1-690, Marcel Dekker, New York 2000.
16. Šámalová J.: Charakterizace mikrostruktury heterogenních materiálů (Characterization of the microstructure of heterogeneous materials, in Czech). Master thesis, ICT Prague 2012.
17. Uhlířová T.: Vysoceporézní celulární keramika připravená biologickým napěňováním (Highly porous cellular ceramics prepared by biological foaming, in Czech). Master thesis, ICT Prague 2013.
18. Uhlířová T., Gregorová E., Pabst W., Veselý M.: Influence of the type and amount of starch on the biological foaming of alumina suspensions, in: *Proceedings of the 9th International Conference on Polysaccharides – Glycoscience*, *Prague (Czech Republic), 6-8 November 2013*, p. 58-63, Ed. Řápková R., Čopíková J., Šárka E., Czech Chemical Society, Prague 2013.
19. Uhlířová T., Gregorová E., Pabst W.: Application of stereological relations for the characterization of porous materials via microscopic image analysis, (contribution 34) in: *Proceedings of the 13th Czech-Slovak Conference (Sborník přednášek) "Přínos metalografie pro řešení výrobních problémů" (Contribution of Metallography to Solving of Production Troubles), Lázně Libverda (Czech Republic), 17-19 June 2014*, p. 198-205, Ed. Kasl J., Zuna P., Czech Technical University (ČVUT), Prague 2014.
20. Russ J. C., Dehoff R. T.: *Practical Stereology*, 2nd ed., p. 1-109, Kluwer Academic / Plenum Publishers, New York 2000.
21. Saltykov S. A.: *Stereometrische Metallographie* (Stereometric Metallography, in German), p. 1-262, Deutscher Verlag für Grundstoffindustrie, Leipzig 1974.
22. Exner H. E.: Quantitative description of microstructures by image analysis, in: *Characterization of Materials Part II*, p. 281-350, Ed. (vol.) Lifshin E. = Volume 2b of Materials Science and Technology – A Comprehensive Treatment, Ed. (series) Cahn R. W., Haasen P., Kramer E. J., Wiley-VCH, Weinheim 2005.
23. ASTM E 112-96: Standard Test Method for Determining Average Grain Size, ASTM standard norm. ASTM International, West Conshohocken / PA (USA) 1996.
24. Higginson R. L., Sellars C. M.: *Worked Examples in Quantitative Metallography*, p. 9-66, Maney, London 2003.
25. Hilliard J. E.: Estimation of microstructural properties in the presence of anisotropy, in: *Ceramic Microstructures – Their Analysis, Significance, and Production*, p. 53-70 (Chap. 2), Ed. Fulrath R. M., Pask J. A., John Wiley & Sons, New York 1968.
26. Hostaša J., Esposito L., Alderighi D., Pirri A.: Opt. Mater. *35*, 798 (2013).